A Pulse Radiolysis Investigation of the Reactions of $BrO_2\cdot$ with $Fe(CN)_6^{4-}$, Mn(II), Phenoxide Ion, and Phenol

R. J. Field,*[1,2] N. V. Raghavan,[1,3] and J. G. Brummer[1,4]

Radiation Laboratory, University of Notre Dame, Notre Dame, Indiana 46556, and Department of Chemistry, University of Montana, Missoula, Montana 59812 *(Received: September 1, 1981; In Final Form: February 5, 1982)*

The single-electron reductions of $BrO_2\cdot$ by $Fe(CN)_6^{4-}$, phenoxide ion, Mn(II), and phenol have been investigated. The $BrO_2\cdot$ was produced by pulse radiolysis of aqueous solutions of BrO_3^- which also contained one of these reductants. All experiments were carried out at pH 6–12. The reductions by $Fe(CN)_6^{4-}$ and phenoxide ion were rapid and clean and led to the products $Fe(CN)_6^{3-}$ and phenoxy radical. The rate constants for these reductions were found to be, respectively, $(1.9 \pm 0.1) \times 10^9$ and $(2.6 \pm 0.2) \times 10^9$ M^{-1} s^{-1}. The reductions of $BrO_2\cdot$ by Mn(II) and phenol were found to be much slower as well as more complex than the reductions by $Fe(CN)_6^{4-}$ and phenoxide ion. The products were, as expected, Mn(III) and phenoxy radical. However, there was a component of $BrO_2\cdot$ reduction by Mn(II) whose rate did not depend upon [Mn(II)]. Furthermore, the rate of $BrO_2\cdot$ reduction by phenol did not depend at all upon the concentration of phenol. It is suggested that these slower reductions were complicated by the well-known dimerization equilibrium between $BrO_2\cdot$ and Br_2O_4. If the rate of reduction of this dimer by Mn(II) or phenol is comparable to or faster than the rate of its return to $BrO_2\cdot$, then the dimerization process itself will become partially or completely rate determining; thus the less than expected dependence of the rates of these reductions on reductant concentrations may be rationalized. Regardless of the exact mechanism of the process, it was shown that the reduction of $BrO_2\cdot$ by Mn(II) and phenol proceeds with the stoichiometry and overall time scale inferred from studies of the reduction of BrO_3^- by some weak metal-ion reductants [including Mn(II)] and of catalyzed (Belousov–Zhabotinsky reaction) and uncatalyzed bromate-driven chemical oscillators.

Introduction

The free-radical species bromine dioxide ($BrO_2\cdot$) is of pivotal importance in the mechanism[5] of the autocatalytic reduction in strongly acid, aqueous media of bromate ion (BrO_3^-) by certain metal ions[6] and metal-ion complexes.[7,8] Some important features of this mechanism are summarized by reactions 1–4 where X^{n+} is the reductant and

$$HBrO_2 + BrO_3^- + H^+ \rightarrow Br_2O_4 + H_2O \quad (1)$$

$$Br_2O_4 \rightleftharpoons 2BrO_2\cdot \quad (2, -2)$$

$$2BrO_2\cdot + 2X^{n+} + 2H^+ \rightarrow 2HBrO_2 + 2X^{(n+1)+} \quad (3)$$

$$HBrO_2 + HBrO_2 \rightarrow HOBr + H^+ + BrO_3^- \quad (4)$$

$X^{(n+1)+}$ is the oxidized product. Some reductants for which this mechanism is important[5-8] are Ce(III), Mn(II), Np(V), $Fe(II)(Phen)_3^{2+}$, and $Ru(II)(bpy)_3^{2+}$. These are all relatively weak, single-electron reductants with reduction potentials greater than 1 V. Bromate ion is a relatively poor single-electron oxidant while $BrO_2\cdot$ is a rather strong one.[5] Noyes[9] has estimated the single-electron reduction potential of $BrO_2\cdot$ to be very close to 1.33 V. Thus the complex, sharply autocatalytic mechanism of reactions 1–4 is dominant over the simple oxygen-transfer (two-electron reduction) mechanism which occurs[10] with stronger single-electron reductants such as $Fe(CN)_6^{4-}$. A detailed mechanism based upon reactions 1–4 has been used to qualitatively explain[11] the reaction of Ce(III) with BrO_3^-. Furthermore, this sequence of reactions forms a critical portion of a mechanism[12] which qualitatively accounts for[13] the remarkable behavior of the oscillatory Belousov–Zhabotinsky reaction.[14]

Even though this mechanism has been remarkably successful in rationalizing a rather large body of experimental fact, its form and values of the rate constants for particular component reactions have mainly been inferred[5,11-13] from the kinetics of complex systems. Thus we have undertaken a direct pulse radiolysis investigation of $BrO_2\cdot$ and reaction 3 with the reductants $Fe(CN)_6^{4-}$, Mn(II), phenoxide ion (PhO^-), and phenol (PhOH). The $BrO_2\cdot$ was produced radiolytically by reaction of the hydrated electron, e_{aq}^-, with BrO_3^-. The reaction[11] of Ce(III) with BrO_3^- and the Belousov–Zhabotinsky reaction[12,14] with cerium as the metal-ion catalyst are the most thoroughly investigated systems where the mechanism of reactions 1–4 is believed to be important. Thus, it would be very desirable to include Ce(III) among the reductants investigated here. Unfortunately, $BrO_2\cdot$ has the potential[9,12] to oxidize Ce(III) to Ce(IV) only in solutions approaching 1 M H_2SO_4. Under these conditions not only is the thermal reaction between Ce(III) and BrO_3^- rapid[6] but also the primary radiolytic species are reactive with H^+ or HSO_4^-. Cerium(III) was found, not unexpectedly, to be unreactive with $BrO_2\cdot$ in neutral solutions. However, the reaction of Mn(II) with BrO_3^- is very similar[5,6] mechanistically to the

(1) Radiation Laboratory, University of Notre Dame.
(2) Department of Chemistry, University of Montana.
(3) Travenol Laboratories, 6301 Lincoln Av., Morton Grove, IL 60053.
(4) Department of Chemistry, Washington State University, Pullman, WA 99164.

(5) Noyes, R. M.; Field, R. J.; Thompson, R. C. *J. Am. Chem. Soc.* **1971**, *93*, 7315.
(6) Thompson, R. C. *J. Am. Chem. Soc.* **1971**, *93*, 7315.
(7) Körös, E.; Burger, M.; Kis, *A. React. Kinet. Catal. Lett.* **1974**, *1*, 475.
(8) Demas, J. N.; Diemente, D. *J. Chem. Educ.* **1973**, *50*, 357.
(9) Noyes, R. M. *J. Am. Chem. Soc.* **1980**, *102*, 4644.
(10) Birk, J. P.; Kozub, S. G. *Inorg. Chem.* **1973**, *12*, 2460.
(11) Barkin, S.; Bixon, M.; Noyes, R. M.; Bar-Eli, K. *Int. J. Chem. Kinet.* **1977**, *11*, 841.
(12) Field, R. J.; Körös, E.; Noyes, R. M. *J. Am. Chem. Soc.* **1972**, *94*, 8649.
(13) Edelson, D.; Noyes, R. M.; Field, R. J. *Int. J. Chem. Kinet.* **1979**, *11*, 155.
(14) Field, R. J. "Theoretical Chemistry: Advances and Perspectives"; Eyring, H.; Henderson, D. Ed.; Academic Press: New York, 1978; Vol. 4, Chapter 2.

0022-3654/82/2086-2443$01.25/0

reaction of Ce(III) with BrO_3^-, and Mn(II) can also serve as the metal-ion catalyst[14] in the Belousov–Zhabotinsky reaction. We believe that our results with Mn(II) in neutral solution can be qualitatively extrapolated to the acidic Ce(III) system. The reaction of $BrO_2\cdot$ with PhOH was included because of its proposed involvement in a mechanism[15,16] of a recently discovered class of uncatalyzed, bromate-driven oscillators.[17] Ferrocyanide ion ($Fe(CN)_6^{4-}$) was included as a test of the method as the radiation chemistry of $Fe(CN)_6^{4-}$ and $Fe(CN)_6^{3-}$ is well understood.[18] Phenoxide ion (PhO^-) was included as part of the work on PhOH.

Experimental Section

The $K_4Fe(CN)_6\cdot 3H_2O$, $MnSO_4\cdot 4H_2O$, $Ce(NH_4)_2(NO_3)_5\cdot 4H_2O$, PhOH, KOH, and $KBrO_3$ used were all Baker Analyzed Reagent grade. All except for $KBrO_3$ were used without further purification. The $KBrO_3$ contained about 0.1% Br^- which was removed by successive slurrying with methyl alcohol[19] until the spectrum[20] of Br_2^- was no longer observed upon the pulse radiolysis of N_2O-saturated solutions of 4×10^{-3} M $KBrO_3$. This is the concentration of $KBrO_3$ used in most of the pulse radiolysis experiments with added reductant, and the absence of such a spectrum indicated that [Br^-] in these experiments was less than 10^{-8} M.

Pulse radiolysis experiments were carried out with fresh solutions prepared from water purified by a Millipore-Milli-Q system. With the exceptions noted in the text, all experiments were carried out in N_2-saturated solutions at natural pH. Dosimity was carried out with SCN^-. All of the reductants undergo a thermal reaction with BrO_3^- which is accelerated by higher acidity. The concentrations of reductant and bromate and the pH were adjusted to suppress such reaction on the hour or so time scale of a set of pulse radiolysis experiments. This requirement often limited the range of reductant concentrations as well as pH over which experiments could be carried out. In all experiments the pH was in the range 6–12.

Pulse radiolysis experiments were carried out at 20 °C with 9-MeV electrons from an ARCO LP-7 linear accelerator. The pulses were of 5–10-ns duration, and the concentration of radicals produced was generally in the range 2–4 μM. Optical detection and signal averaging were carried out by a computer system described elsewhere.[21] The extinction coefficient of $BrO_2\cdot$ is small enough ($\epsilon_{max} \simeq 1000$ M^{-1} cm^{-1}) that at least 30 averaged pulses were usually necessary to obtain usable data.

Numerical Simulation Techniques. The data resulting from many of the experiments reported here were too complex to be interpreted by conventional techniques. This complexity resulted mainly from the fact that radiolytically produced HO· usually reacted with added reductants in a manner analogous to that of $BrO_2\cdot$ in reaction 3. Furthermore, scavenging of HO· by *tert*-butyl alcohol introduced additional complications in longer time scale reactions. Thus numerical simulation techniques[22] were used for data analysis. These simulations were carried out by numerical integration of the set of ordinary differential equations resulting from application of the law of mass action[23] to the set of elementary reactions believed to be reponsible for the overall chemical change. A robust, stiffly stable numerical integrator due to Hindmarsh[24] was used even though stiffness was not usually a problem in this work. Numerical simulation methods are particularly useful in radiation chemistry because a very large number of critically evaluated rate constant values are available[25] for the reactions of HO· and e_{aq}^-. Thus it was often possible to design experiments such that there was only one rate constant whose value could be adjusted to give good agreement between experiment and simulation. Such unambiguously determined rate constant values were then used in all further simulations.

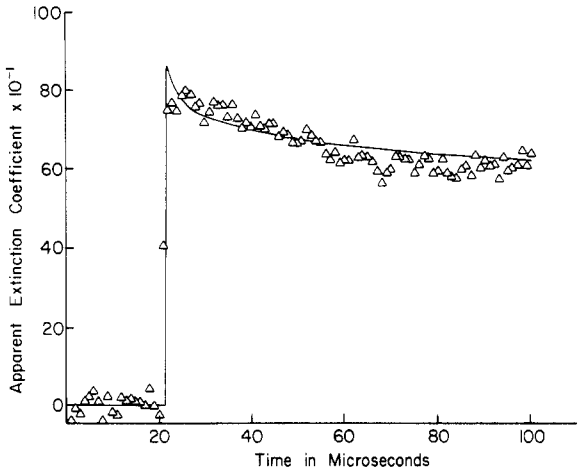

Figure 1. Apparent extinction coefficient at 480 nm vs. time in microseconds of $BrO_2\cdot$ resulting from pulse radiolysis of a N_2-saturated solution of 4.19×10^{-3} M $KBrO_3$ at natural pH. The Δ are experimental data and the solid line is a simulation based upon the reactions in Table I labeled a.

Results and Discussion

Radiation Chemistry of BrO_3^- and the Properties of $BrO_2\cdot$. Buxton and Dainton (BD)[26] have investigated the radiation chemistry of basic, aqueous solutions of BrO_3^-, and our results in neutral solution agree qualitatively with theirs. This chemistry can be summarized by reactions 5–8. The numbers in parentheses in reaction 5 are the

$$H_2O \rightarrow HO\cdot\ (2.65),\ e_{aq}^-\ (2.6),\ H\cdot\ (0.6) \qquad (5)$$

$$H_2O + BrO_3^- + e_{aq}^- \rightarrow \{BrO_3^{2-}\} \rightarrow BrO_2\cdot + 2HO^- \qquad (6)$$

$$BrO_2\cdot + BrO_2\cdot \rightleftarrows Br_2O_4 \qquad (-2, 2)$$

$$HO^- + Br_2O_4 \rightarrow H^+ + BrO_3^- + BrO_2^- \qquad (7)$$

$$HO\cdot + BrO_2\cdot \rightarrow H^+ + BrO_3^- \qquad (8)$$

yields (G) of the various primary radiolytic species.[31] Upon pulse radiolysis of a BrO_3^- solution, a transient species appeared with a featureless absorption spectrum[20,26] centered upon 480 nm where the extinction coefficient was 1000 ± 100 M^{-1} cm^{-1}. Buxton and Dainton[26] demonstrated

(15) Orbán, M.; Körös, E.; Noyes, R. M. *J. Phys. Chem.* **1979**, *83*, 212.
(16) Herbine, P.; Field, R. J. *J. Phys. Chem.* **1980**, *84*, 1330.
(17) Orbán, M.; Körös, E. *J. Phys. Chem.* **1979**, *83*, 212.
(18) Waltz, W. L.; Akhtar, S. S.; Eager, R. L. *Can. J. Chem.* **1973**, *51*, 2525.
(19) Graziani, K. R.; Hudson, J. L.; Schmitz, R. A. *Chem. Eng. J.* **1976**, *12*, 9.
(20) Hug, G. *Natl. Stand. Ref. Data Ser., Natl. Bur. Stand.* **1981**.
(21) (a) Patterson, L. K.; Lillie, J. *Int. J. Radiat. Phys. Chem.* **1974**, *6*, 129. (b) Schuler, R. H.; Neta, P.; Zemel, H.; Fessenden, R. W. *J. Am. Chem. Soc.* **1976**, *98*, 3825.
(22) "Symposium on Reaction Mechanisms, Models, and Computers" *J. Phys. Chem.* **1977**, *25*.
(23) Moore, W. J. "Physical Chemistry"; Prentice-Hall: Englewood Cliffs, NJ, 1972; p 281.
(24) Hindmarsh, A. C. "Gear: Ordinary Differential Equation Solver", Technical Report No. UCID-3001, Rev. 2, Lawrence Livermore Laboratory, 1972, based upon Gear, C. W. *Comm. ACM.* **1971**, *14*, 185.
(25) (a) Anbar, M.; Bambenek, M.; Ross, A. B. *Natl. Stand. Ref. Data Ser., Natl. Bur. Stand.* **1973**, *No. 43*. (b) Farhataziz; Ross, A. B. *Ibid.* **1977**, *No. 59*.
(26) Buxton, G. V.; Dainton, F. S. *Proc. R. Soc. London, Ser. A* **1968**, *304*, 427.

TABLE I: Reactions and Rate Constants Used in Simulations

no.[a]	reaction	rate constant, M^{-1} s^{-1}	ref	simulations used in
	$e_{aq}^- + e_{aq}^- + 2H_2O \rightarrow H_2 + 2HO^-$	6×10^9	25a	a-e
	$e_{aq}^- + H_2O \rightarrow H\cdot + HO^-$	16	25a	a-e
	$e_{aq}^- + HO\cdot \rightarrow HO^-$	3×10^{10}	25a	a-e
	$e_{aq}^- + N_2O + H_2O \rightarrow HO\cdot + HO^- + N_2$	8.7×10^9	25a	a-e
	$e_{aq}^- + Mn(II) \rightarrow Mn(I)$	8×10^7	25a	d
	$e_{aq}^- + PhO^- \rightarrow PhO^{2-}$	4×10^6	25a	c
	$e_{aq}^- + PhOH \rightarrow PhOH^-$	2×10^7	25a	e
6	$e_{aq}^- + BrO_3^- + H_2O \rightarrow BrO_2\cdot + 2HO^-$	3×10^9	25a	a-e
	$HO\cdot + HO\cdot \rightarrow H_2O_2$	6×10^9	25b	a-e
11	$HO\cdot + Fe(CN)_6^{4-} \rightarrow HO^- + Fe(CN)_6^{3-}$	1×10^{10}	25b	b
17	$HO\cdot + Mn(II) \rightarrow HO^- + Mn(III)$	2×10^8	25b	d
13	$HO\cdot + PhO^- \rightarrow HO^- + PhO\cdot$	4.5×10^9	here	c
20	$HO\cdot + PhOH \rightarrow H_2O + PhO\cdot$	2.1×10^9	here	e
18	$HO\cdot + PhOH \rightarrow Ph(OH)_2\cdot$	4.5×10^9	here	e
19	$Ph(OH)_2\cdot \rightarrow PhO\cdot + H_2O$	8.0×10^4 (s^{-1})	here	e
14	$PhO\cdot + PhO\cdot \rightarrow (PhO)_2$	3.0×10^8	here	e
8	$HO\cdot + BrO_2\cdot \rightarrow BrO_3^- + H^+$	2.0×10^9	here	a-e
9	$HO\cdot + BrO_3^- \rightarrow HO^- + BrO_3\cdot$	4×10^6	25b	a-e
2	$Br_2O_4 \rightarrow BrO_2\cdot + BrO_2\cdot$	3.1×10^5 (s^{-1})	here	a-e
−2	$BrO_2\cdot + BrO_2\cdot \rightarrow Br_2O_4$	6.0×10^9	here	a-e
10	$BrO_2\cdot + Fe(CN)_6^{4-} \rightarrow BrO_2^- + Fe(CN)_6^{3-}$	1.9×10^9	here	b
12	$BrO_2\cdot + PhO^- \rightarrow BrO_2^- + PhO\cdot$	2.6×10^9	here	c, e
15	$BrO_2\cdot + Mn(II) \rightarrow BrO_2^- + Mn(III)$	$\sim 1.5 \times 10^6$	here	d
16	$BrO_2\cdot + PhOH \rightarrow BrO_2^- + PhO\cdot$	$\sim 3.0 \times 10^5$	here	e
22	$Br_2O_4 + Mn(II) \rightarrow BrO_2\cdot + BrO_2^- + Mn(III)$	$\sim 1.0 \times 10^8$	here	d
23	$Br_2O_4 + PhOH \rightarrow BrO_2\cdot + BrO_2^- + PhO\cdot$	$\geqslant 5.0 \times 10^8$	here	e

[a] Reaction numbers refer to text. Reaction used in simulations with (a) no added reductant, (b) $Fe(CN)_6^{4-}$ as reductant, (c) PhO^- as reductant, (d) Mn(III) as reductant, (e) PhOH as reductant.

that this species must be $BrO_2\cdot$. Försterling et al. observed a very similar spectrum both as an intermediate[27] during the reaction of Ce(III) with BrO_3^- and as a product in a direct investigation[28] of reactions 1, 2, and 4. They assigned this spectrum to $BrO_2\cdot$. Barat et el.[29] observed an identical spectrum ($\epsilon_{480} = 990 \pm 50$ M^{-1} cm^{-1}) resulting from the flash photolysis of BrO_3^-, and they assigned it to $BrO_2\cdot$. Thus the spectrum of $BrO_2\cdot$ is well-known. Figure 1 shows the time-resolved apparent extinction coefficient at 480 nm vs. time obtained by pulse radiolysis of a solution containing only BrO_3^-. An apparent extinction coefficient is calculated by assuming that the entire yield of the radiolytic precursor is converted to the absorbing species. There is no detectable delay between the disappearance of e_{aq}^- and the appearance of $BrO_2\cdot$. Thus the species BrO_3^{2-} appearing in reaction 6 can live for no longer than a few hundred nanoseconds. Reaction 9 is

$$BrO_3^- + HO\cdot \rightarrow BrO_3\cdot + HO^- \qquad (9)$$

relatively slow[25b] and neither we nor BD find strong evidence of it. Reaction 2, −2, an equilibrium between $BrO_2\cdot$ and its dimer, Br_2O_4, was proposed by BD to rationalize the fact that with no added reducing substrate $BrO_2\cdot$ disappeared in two stages. These were an initial rapid stage in which nearly half of the $BrO_2\cdot$ disappeared according to approach to equilibrium kinetics of the form suggested by reaction 2, −2 followed by a second stage which lasted about 100 times longer. They reported a value of $K_2 = k_2/k_{-2} \simeq 19$ M^{-1}. However, we calculate from BD's data that $K_2 \simeq 19000$ M^{-1}. This latter value reproduces BD's data while the former does not. Försterling et al.[28] have also noted this descrepancy. Furthermore, they[28] report a less directly determined value of $K_2 \simeq 7 \times 10^5$ M^{-1} in strongly acid media. The value calculated from BD's data is closer to being correct under the conditions used here than the value due to Försterling et al.;[28] at the concentration of $BrO_2\cdot$ present in our experiments ($\sim 3 \times 10^{-6}$ M) a value of $K_2 = 19000$ M^{-1} predicts that less than 5% of it should be tied up as the dimer. It is barely possible to see such a small effect in the data exhibited in Figure 1. The line in Figure 1 is a simulated based upon the reactions labeled a in Table I and the corresponding rate constants. These imply $K_2 = 19000$ M^{-1}. If the value of K_2 under the experimental conditions used here were as large as that reported by Försterling et al.,[21] a very large fraction of the $BrO_2\cdot$ would quickly be tied up as the dimer. We were unable to produce concentrations of $BrO_2\cdot$ high enough to reproduce BD's experiments because of the limited pulse size of the LINAC as compared to the Van de Graf generator used by BD.

While we were unable to detect a change in $BrO_2\cdot$ concentration resulting from equilibrium 2, we believe that the dimerization of $BrO_2\cdot$ does affect our experiments on the reduction of $BrO_2\cdot$ by Mn(II) and PhOH. Reaction 3 is very rapid with $Fe(CN)_6^{4-}$ or PhO^- as the reductant, and we see no complications. However, with Mn(II) or phenol as the reductant, reaction 3 is much slower than with the former reductants and complications appear which may result from the dimerization of $BrO_2\cdot$.

Buxton and Dainton[26] did not consider reaction 8 as most of their experiments were done in basic solution where reaction 7 is the dominant route for the final removal of $BrO_2\cdot$. However, in neutral or slightly acid solutions such as used here, reaction 8 is the dominant $BrO_2\cdot$ removal route; addition of Ce(III), which reacts rapidly[25b] under these conditions with HO· but not with $BrO_2\cdot$, eliminates the slow decay of $BrO_2\cdot$ evident in Figure 1. The simulation in Figure 1 was carried out by assuming that $k_8 = 2 \times 10^9$ M^{-1} s^{-1}.

Rapid Reduction of $BrO_2\cdot$ by $Fe(CN)_6^{4-}$ and PhO^-. Both of these species react rapidly and cleanly with $BrO_2\cdot$ to give the expected products, $Fe(CN)_6^{3-}$ and phenoxyl radical (PhO·). Reaction 10 was investigated first because the

$$Fe(CN)_6^{4-} + BrO_2\cdot \rightarrow Fe(CN)_6^{3-} + BrO_2^- \qquad (10)$$

(27) Försterling, H. D.; Lamberz, H.; Schreiber, H. *Z. Naturforsch. A* **1980**, *35*, 329.
(28) Försterling, H. D.; Lamberz, H.; Schreiber, H. *Z. Naturforsch. A* **1980**, *35*, 1354.
(29) Barat, F.; Gilles, L.; Hickel, B.; Lesigne, B. *J. Phys. Chem.* **1972**, *76*, 302.

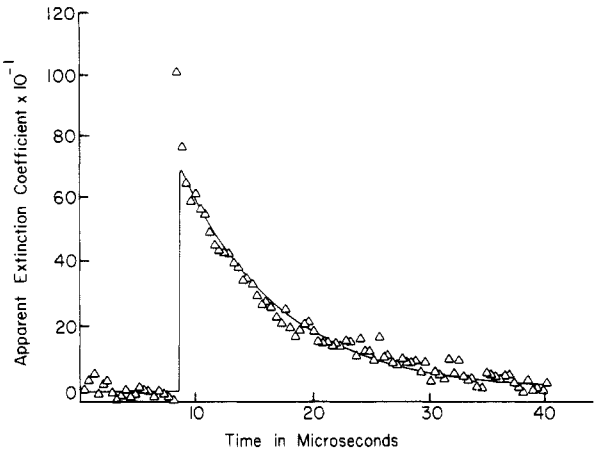

Figure 2. Decay vs. time in microseconds of the apparent extinction coefficient at 480 nm of $BrO_2\cdot$ resulting from pulse radiolysis of a N_2-saturated solution of 4.19×10^{-3} M BrO_3^- and 6.29×10^{-5} M $Fe(CN)_6^{4-}$ at natural pH. The Δ are experimental data and the solid line is a simulation based on the reactions in Table I labeled b.

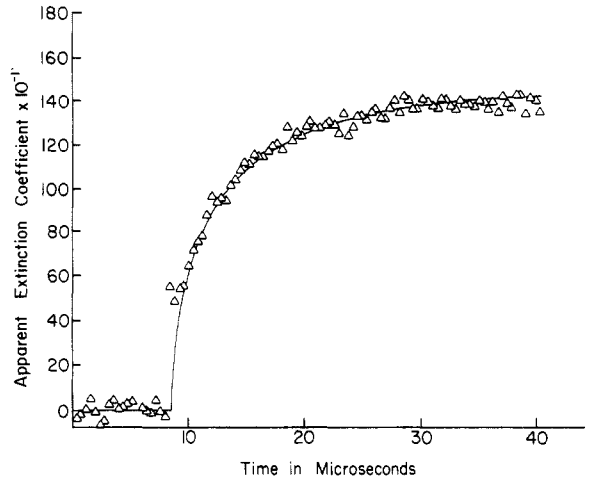

Figure 3. Growth vs. time in microseconds of the apparent extinction coefficient at 420 nm of $Fe(CN)_6^{3-}$ resulting from pulse radiolysis of a N_2-saturated solution of 4.19×10^{-3} M BrO_3^- and 6.29×10^{-5} M $Fe(CN)_6^{4-}$ at natural pH. The Δ are experimental data and the solid line is a simulation based upon the reactions in Table I labeled b.

absorption spectra of the various species involved are well-known and well separated, and the radiation chemistry of $Fe(CN)_6^{4-}$ and $Fe(CN)_6^{3-}$ is well understood.[18] Ferrocyanide ion has no absorption spectrum above 400 nm. The featureless absorption spectra of $Fe(CN)_6^{4-}$ and $BrO_2\cdot$ are centered upon 420 and 480 nm, respectively, and there is little overlap at these wavelengths. In agreement with Försterling et al.,[28] we can detect no absorbance due to BrO_2^- above 400 nm. The concentration of BrO_3^- was 4×10^{-3} M in a typical pulse radiolysis experiment, and the concentration of $Fe(CN)_6^{4-}$ was within a factor of two of 1×10^{-4} M. Experiments were carried out in N_2-saturated solutions at natural pH. The maximum concentrations of $Fe(CN)_6^{4-}$ and BrO_3^- which could be used in a particular experiment were limited by their thermal reaction.[10] Sixteen experiments were carried out with $Fe(CN)_6^{4-}$ concentrations ranging from 6.3×10^{-5} to 1.8×10^{-4} M.

Figures 2 and 3 show the time-resolved behavior at 480 and 420 nm during a typical pulse radiolysis experiment involving $Fe(CN)_6^{4-}$ and BrO_3^-. The absorption at 480 nm due to $BrO_2\cdot$ decays as the absorbance at 420 nm due to $Fe(CN)_6^{3-}$ grows. Experiments were carried out on either side of 420 and 480 nm to demonstrate that the species involved were indeed $Fe(CN)_6^{3-}$ and $BrO_2\cdot$. The growth

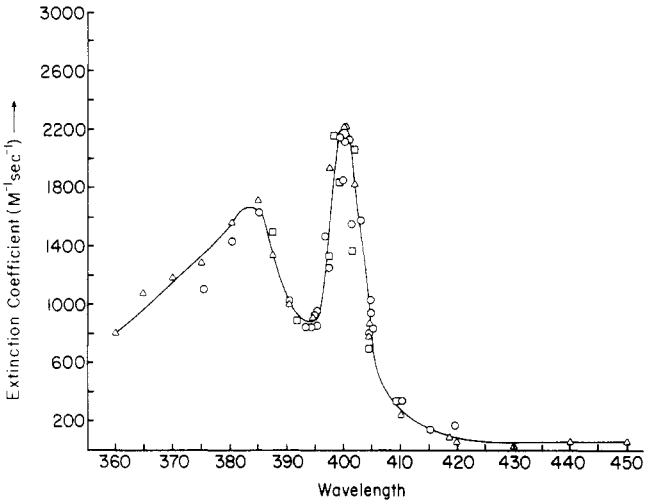

Figure 4. O shows the spectrum of PhO· obtained by pulse radiolysis of a N_2O-saturated solution of 2.66×10^{-4} M PhOH with pH adjusted to 12 with KOH. This is taken to be the authentic spectrum of PhO·. Δ shows the spectrum of the product obtained by pulse radiolysis of a N_2-saturated solution of 4.19×10^{-3} M BrO_3^- and 4.80×10^{-1} M PhO^- with pH adjusted to 12 with KOH. This is the product of reaction 12. □ shows the spectrum of the product obtained by pulse radiolysis of a N_2-saturated solution of 4.19×10^{-3} M BrO_3^- and 5.46×10^{-3} M PhOH at natural pH. This is the product of process 15.

in Figure 3 is complicated by the simultaneous occurrence of reaction 11. The solid lines in Figures 2 and 3 are

$$HO\cdot + Fe(CN)_6^{4-} \rightarrow Fe(CN)_6^{3-} + HO^- \quad (11)$$

simulations based upon a value of $k_{10} = (1.9 \pm 0.1) \times 10^9$ $M^{-1}\ s^{-1}$, the reactions in Table I labeled b, the authentic extinction coefficients of the absorbing species, and the radiolytic yields[31] noted in reaction 5. The value of k_{10} quoted was the only expendable parameter in the simulations, and this value was able to reproduce all of our growth and decay curves with no detectable trend through the concentration range studied. Simulations based upon the same set of parameters quantitatively reproduced experiments in similar solutions saturated with N_2O such that nearly all e_{aq}^- was converted[31] to HO· and reaction 10 was nearly eliminated. There was no evidence of any complexity in these experiments. Reaction 10 was apparently the only reaction removing $BrO_2\cdot$.

Reaction 12 was also found to be rapid and simple. An

$$BrO_2\cdot + PhO^- \rightarrow BrO_2^- + PhO\cdot \quad (12)$$

authentic spectrum of PhO· was obtained by pulse radiolysis of N_2O-saturated solutions of phenol at pH ~12 where PhOH is essentially completely dissociated to PhO^-. Under these conditions e_{aq}^- was converted to HO· and PhO· was produced in reaction 13.[26] The spectrum of PhO· so

$$HO\cdot + PhO^- \rightarrow HO^- + PhO\cdot \quad (13)$$

obtained is exhibited in Figure 4, and it agrees well with that obtained by Land and Ebert.[32] There is very little overlap of the spectra of $BrO_2\cdot$ and PhO·. Experiments on reaction 12 were carried out in N_2-purged solutions adjusted to pH ~12 with KOH and containing 4×10^{-3} M BrO_3^-. Eighteen experiments were carried out in which the concentration of PhO^- was varied from 4.7×10^{-5} to 1.78×10^{-4} M. Figure 4 shows that the spectrum of the product obtained in these experiments agrees very well

(30) Davies, G.; Kirschenbaum, L.; Kustin, K. *Inorg. Chem.* **1968**, *7*, 146.
(31) Dragonic, I. G.; Dragonic, Z. D. "The Radiation Chemistry of Water"; Academic Press: New York, 1971.
(32) Land, E. J.; Ebert, M. *Trans. Faraday Soc.* **1967**, *63*.

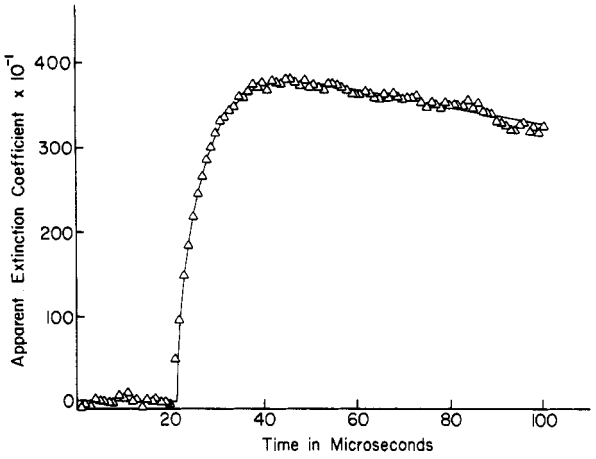

Figure 5. Growth vs. time in microseconds of the apparent extinction coefficient at 402 nm of PhO· resulting from the pulse radiolysis of a N_2-saturated solution of 4.19×10^{-3} M BrO_3^- and 4.70×10^{-5} M PhO^- with pH adjusted to 12 with KOH. The Δ are experimental data and the solid line is a simulation based upon the reactions in Table I labeled c.

with that of PhO·, and Figure 5 shows the growth of absorbance due to this species at 402 nm. The decay at longer times in Figure 5 is apparently due to reaction 14.

$$PhO\cdot + PhO\cdot \rightarrow (PhO)_2 \qquad (14)$$

The solid line in Figure 5 is a simulation based upon $k_{12} = (2.6 \pm 0.2) \times 10^9$ M^{-1} s^{-1}, $k_{14} = (3 \pm 0.5) \times 10^8$ M^{-1} s^{-1}, the reactions in Table I labeled c, the authentic extinction coefficients of all species involved, and the radiolytic yields noted in reaction 5. Even though there were two expendable parameters in these simulations, k_{12} and k_{14}, the two reactions involved were important on different time scales, and their effects were easily separable. The quoted rate constant values were able to simulate all growth and decay curves, and there was no detectable trend in either rate constant value over the concentration range studied. As in the $Fe(CN)_6^{4-}$ experiments, there was no evidence of further complexity.

Slower Reductions of BrO_2· by Mn(II) and PhOH. Processes 15 and 16 were found to be substantially slower

$$BrO_2\cdot + Mn(II) \rightarrow BrO_2^- + Mn(III) \qquad (15)$$

$$BrO_2\cdot + PhOH \rightarrow BrO_2^- + PhO\cdot + H^+ \qquad (16)$$

than reactions 10 and 12, and they are apparently complex. Process 15 will be discussed first. The absorption spectra of BrO_2· and Mn(III) are both centered near 480 nm. However, the extinction coefficient of Mn(III) is about 10 times less than that of BrO_2·. This quantity was determined by pulse radiolysis of N_2O-saturated solutions containing Mn(II) ion. Reaction 17 is the only source of

$$Mn(II) + HO\cdot \rightarrow Mn(III) + HO^- \qquad (17)$$

Mn(III) under these conditions. The value obtained at 480 nm is about 100 M^{-1} cm^{-1} and agrees with that of Davies et al.[30] Figure 6 shows a typical experiment with Mn(II) as the reductant. The initial absorbance at 480 nm due to BrO_2· decays to a plateau due to Mn(III). Even though the results in Figure 6 were obtained at one of the highest Mn(II) concentrations used, the time scale in Figure 6 is 5–10 times longer than the time scales of Figures 2, 3, and 5 where $Fe(CN)_6^{4-}$ or PhO^- were used as reductants. Such long time scale experiments with Mn(III) might be expected to be even cleaner than the rapid reductions of $Fe(CN)_6^{4-}$ or PhO^- because nearly all of the radiolytic HO· is consumed in reaction 17 before process 15 occurs to any appreciable extent. Thus the only species expected to be

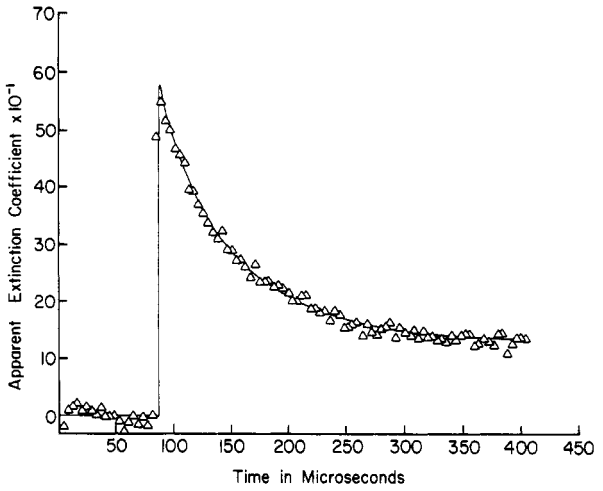

Figure 6. Decay vs. time in microseconds of the apparent extinction coefficient at 480 nm of BrO_2· resulting from pulse radiolysis of a N_2-saturated solution of 4.19×10^{-3} M BrO_3^- and 8.13×10^{-3} M Mn(II) at natural pH. The Δ are experimental data and the solid line is a simulation based upon the reactions in Table I labeled d.

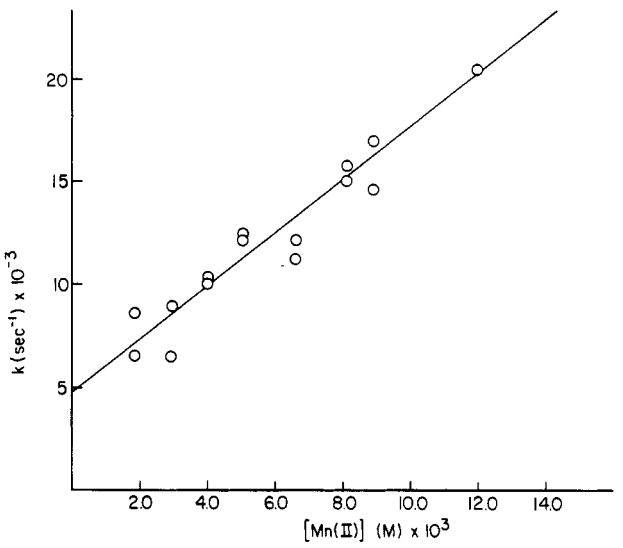

Figure 7. Plot vs Mn(II) concentration of the pseudo-first-order rate constants for the decay of the apparent extinction coefficient at 480 nm of BrO_2· in the presence of Mn(II) in the concentration range 1.86×10^{-3} to 1.20×10^{-2} M.

present during the bulk of an experiment such as that in Figure 6 are the participants in process 15. This expected simplicity did not materialize. Fifteen experiments were carried out with [Mn(II)] in the range of 1.86×10^{-3} to 1.20×10^{-2} M. Figure 7 shows a plot vs [Mn(II)] of pseudo-first-order rate constants obtained from the BrO_2· decay curves resulting from these experiments. While there is a linear dependence of pseudo-first-order rate constants on [Mn(II)], there is also an intercept which suggests that BrO_2· disappears both by an elementary reaction of the form of process 15 and also by a process less than first order in [Mn(II)]. The yield of Mn(III) obtained, however, indicates that both processes have the stoichiometry of process 15. Each experiment with Mn(II) as reductant could be reproduced individually by numerical simulation based upon an elementary reaction of the form of process 15 being the only route by which Mn(II) can reduce BrO_2·. However, the values of k_{15} obtained from these simulations decreased linearly as [Mn(II)] increased.

The phenomenon with Mn(II) as reductant displayed in Figure 7 reached its natural conclusion when PhOH was used as the reductant. In these experiments the rate of decay of BrO_2· did not depend at all upon [PhOH].

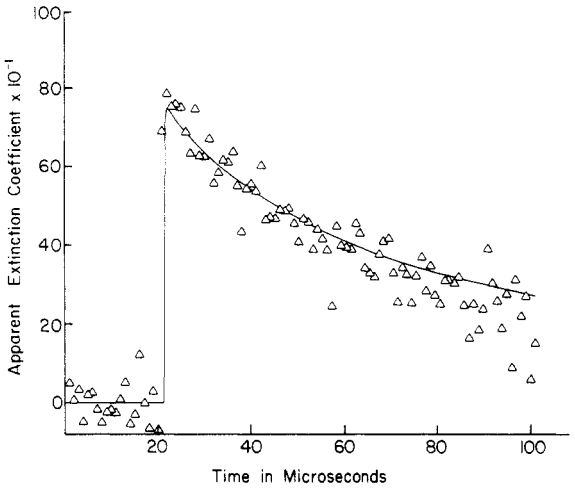

Figure 8. Decay vs. time in microseconds of the apparent extinction coefficients at 480 nm of $BrO_2\cdot$ resulting from pulse radiolysis of a N_2-saturated solution of 4.19×10^{-3} M BrO_3^- and 5.69×10^{-3} M PhOH at natural pH. The Δ are experimental data and the solid line is a simulation based upon the reactions in Table I labeled e.

However, the stoichiometry of process 16 was followed. A species with the spectrum of PhO· (see Figure 4) appeared on the same time scale as the decay of $BrO_2\cdot$. Figure 8 shows the results at 480 nm of an experiment at a [PhOH] of 5.69×10^{-3} M. The growth of PhO· at 402 nm was also monitored. Experiments were carried out with phenol concentrations ranging from 5.69×10^{-3} to 1.88×10^{-2} M. Even though [PhOH] increased by a factor of 3.33 in these experiments, the pseudo-first-order rate constant for the decay of $BrO_2\cdot$ remained essentially unchanged at about 1.65×10^4 s^{-1}. The concentration of PhO^- in equilibrium PhOH was not high enough in our experiments to completely account for the observed decay of $BrO_2\cdot$, although it certainly contributes. In our unbuffered experiments [PhO^-] increases at the square root of [PhOH], and so this suggestion cannot account for the zero-order dependence on [PhOH] of $BrO_2\cdot$ disappearance.

The experiments with PhOH were more difficult to interpret than those with Mn(II) because of the complexity[32] of the interaction of radiolytically produced HO· with PhOH. The PhO· growth curves obtained are, for the same reason, more difficult to interpret than the $BrO_2\cdot$ decay curves. We have investigated the interaction of radiolytic HO· with PhOH under the conditions of pH, dose, and PhOH concentration used in our $BrO_2\cdot$ reduction experiments, but without BrO_3^-, and our conclusions generally agree with those of Land and Ebert[32] obtained under somewhat different conditions. More than half of the HO· adds to PhOH according to reaction 18. The product of

$$PhOH + HO\cdot \rightarrow Ph(HO)_2\cdot \quad (18)$$

this addition, dihydroxycyclohexadienyl radical ($Ph(OH)_2\cdot$), then dehydrates according to reaction 19 to give

$$Ph(OH)_2\cdot \rightarrow PhO\cdot + H_2O \quad (19)$$

PhO·. The spectrum of $Ph(OH)_2\cdot$ has a maximum at 330 nm and does not overlap that of PhO· or $BrO_2\cdot$. Unlike Land and Ebert, however, we found a substantial amount of direct hydrogen atom abstraction from PhOH by HO· to give PhO· according to reaction 20. The rate constants

$$HO\cdot + PhOH \rightarrow PhO\cdot + H_2O \quad (20)$$

for reactions 18–20 listed in Table I were determined by us in N_2O-saturated solutions containing only PhOH. These rate constants generally agree with those of Land Ebert[32] and were used in simulations of experiments involving both BrO_3^- and PhOH.

The results of these experiments on the reduction of $BrO_2\cdot$ by Mn(II) and PhOH imply that there are reactions leading to the stoichiometries of processes 15 and 16 for which the rate-determining step does not involve the reductant. Because the phenomenon occurs in both the experiments with Mn(II) and with PhOH, it seems unlikely that it is specific to the reductant, and probably involves $BrO_2\cdot$ itself. An obvious explanation is reaction 21 followed

$$BrO_2\cdot + BrO_3^- \rightarrow BrO_3\cdot + BrO_2^- \quad (21)$$

by the rapid conversion of $BrO_3\cdot$ to BrO_3^- by the reductant. However, the electron affinity of $BrO_3\cdot$ is substantially greater[26] than that of $BrO_2\cdot$. Furthermore, the rate of decay of $BrO_2\cdot$ in the PhOH and Mn(II) experiments did not change when [BrO_3^-] was doubled.

The only scheme that is apparent to us to rationalize these results is to invoke the dimerization of $BrO_2\cdot$, reaction −2, followed by reaction of the dimer, Br_2O_4, with the reductant according to reactions 22 and 23. If reaction

$$Br_2O_4 + Mn(II) \rightarrow BrO_2^- + BrO_2\cdot + Mn(III) \quad (22)$$

$$Br_2O_4 + PhOH \rightarrow HBrO_2 + BrO_2\cdot + PhO\cdot \quad (23)$$

23 is fast compared to reaction 2, then the dimerization of $BrO_2\cdot$, reaction −2, will be rate determining and this rationalizes the independence of the rate of reaction of $BrO_2\cdot$ with PhOH on [PhOH]. The reaction with Mn(II) is apparently an intermediate case. Numerical simulation including reactions 22 and 23 reproduced all of our experiments on the reduction of $BrO_2\cdot$ by PhOH and Mn(II). The solid line in Figures 7 and 8 result from such simulations. There was no trend in rate constant values derived from the simulations as the concentration of the reductants were varied. These rate constant values are $k_{-2} = 6.0 \times 10^9$ M^{-1} s^{-1}, $k_{15} = 1.5 \times 10^6$ M^{-1} s^{-1}, $k_{22} = 1 \times 10^8$ M^{-1} s^{-1}, $k_{16} = 3 \times 10^5$ M^{-1} s^{-1}, and $k_{23} \geq 5 \times 10^8$ M^{-1} s^{-1}. All of these rate constant values are dependent upon the assumed value of k_2 and are uncertain to the extent that this parameter is. There are, however, problems with this interpretation. The value of k_2 resulting from the simulations is about 4 times larger than the value reported by BD.[26] Furthermore, it is not apparent why Br_2O_4 should be reduced by Mn(II) and PhOH faster than $BrO_2\cdot$ itself. Indeed, it seems as though the converse should be true. An obvious test of the proposed scheme is to determine whether the decay of $BrO_2\cdot$ in the PhOH experiments is second order in [$BrO_2\cdot$] as it should be if reaction −2 is rate determining. Unfortunately, because of the relatively poor precision of the data, particularly in the important later stages of the decay where the absorbance is very low, it is not possible for us to make a clear determination of the order of the decay of $BrO_2\cdot$. Both first- and second-order plots appear equally linear, and it was not experimentally convenient to vary the initial concentration of $BrO_2\cdot$ over a very wide range.

We have neglected in our simulations the removal of $BrO_2\cdot$ through oxidation by Mn(III) or PhO·, reactions 24 and 25. Both of these reactions are expected to be favored

$$Mn(III) + BrO_2\cdot + H_2O \rightarrow Mn(II) + BrO_3^- + 2H^+ \quad (24)$$

$$PhO\cdot + BrO_2\cdot + H_2O \rightarrow PhOH + BrO_3^- + H^+ \quad (25)$$

thermodynamically, and they can rationalize the less than first-order dependence on [Mn(II)] and [PhOH] of the rate of $BrO_2\cdot$ decay. This is so because both Mn(III) and PhO· are produced by HO· from the pulse, and the amounts produced are related to the pulse size rather than to the concentration of reductant. However, the concentrations

of Mn(III) and PhO· produced in this manner were always at least 1000 times less than the concentration of the reductant. Thus for these reactions to be the cause of the observed BrO_2· decay k_{24} would have to be nearly 10^9 M^{-1} s^{-1} and k_{25} nearly 10^7 M^{-1} s^{-1}. These rate constant values seem absurdly high for such complex reactions. Furthermore, these reactions do not lead to the observed stoichiometries, i.e., PhO· appears as BrO_2· decays rather than disappearing. Barkin et al.[11] estimate k_{24} with Ce(IV) to be about 10 M^{-1}, and Mn(III) is expected to behave similarly.[5,6]

Conclusion

Even though there are reservations concerning the exact mechanistic details of processes 15 and 16, the original goal of this work has been accomplished. We have directly demonstrated that BrO_2· is reduced by Mn(II) and PhOH and that the products of these reactions are indeed Mn(III) and PhO·. Furthermore, the overall rates of these reactions are just about those inferred from simulations of the metal-ion-catalyzed Belousov–Zhabotinsky reaction[13] and the uncatalyzed bromate oscillator involving PhOH.[16] We point out that the results obtained here are for nearly neutral pH while the former results were obtained in strongly acid media.

Acknowledgment. The research described here was partially supported by the Office of Basic Energy Sciences of the Department of Energy and by the National Science Foundation under graint CHE-8023755. This is document No. NDRL-2264 of the University of Notre Dame Radiation Laboratory. We thank the University of Montana Computer Center for computing time, and Professor John Barr for technical assistance.

Resonance Raman Spectra of the Tautomers of Pyridoxal and Salicylaldehyde Schiff Bases

John W. Ledbetter

Department of Biochemistry, Medical University of South Carolina, Charleston, South Carolina 29425 *(Received: December 8, 1981; In Final Form: February 23, 1982)*

Resonance Raman spectra of pyridoxal 5′-phosphate and salicylaldehyde Schiff bases of amino acids in H_2O show the presence of the $-C{=}NH^+$ bond. This proves that the predominant resonance form of the tautomer is the protonated imine. The tautomer of aryl Schiff bases in less polar solvents exists as the quinoid resonance structure.

Introduction

In alcoholic solvents Dudek and Dudek[1] demonstrated with ^1H NMR spectra that the Schiff bases of salicylaldehyde (I) undergo a proton transfer from the hydroxyl

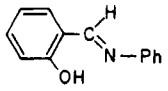

I, 335 nm

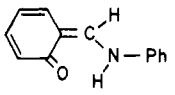

II, 430 nm

group to the imine group. The resulting structure was shown as a quinoid molecule (II). Electronic absorption studies[2,3] indicated that in a variety of protonic solvents a band about 430 nm is caused by a proton tautomerism. The λ_{max} of the band for the Schiff bases depended on the structure and solvent.[4,5]

The amino acid Schiff bases of pyridoxal 5′-phosphate (PLP) also exhibit an absorption band about 413 nm in aqueous solutions and about 430 nm in many PLP-dependent enzymes. Assignment of the band in biochemical literature[6] is usually made to tautomer III which is as-

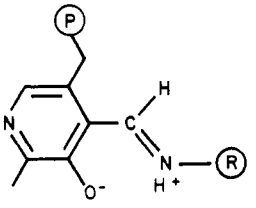

III

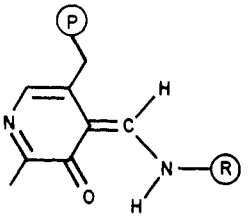

IV

sumed always in resonance with IV. This assignment is largely due to the work of Heinert and Martell[7-9] who observed bands at 1625–1650 and about 1510 cm^{-1} in the infrared spectra of the Schiff bases in KBr. The assignment of the former band to an amide I carbonyl stretching vibration and the latter to a conjugated amide vibration led them to conclude that the proton tautomer (III ↔ IV) was responsible for the absorption about 422 nm. Ledbetter[10] also observed bands at 1640 and 1525–1547 cm^{-1} in the spectra of salicylidene anils in KBr and alcohols. Assignment was to the carbonyl stretching frequency and to the vinyl stretch of the enamine proton tautomer (II).

There remains, nevertheless, identification of the most prevalent resonance structure of PLP Schiff bases in water

(1) G. O. Dudek and E. P. Dudek, *J. Am. Chem. Soc.*, **88**, 2407 (1966).
(2) J. D. Margerum and J. A. Sousa, *Appl. Spectrosc.*, **19**, 91 (1965).
(3) J. W. Ledbetter, *J. Phys. Chem.*, **70**, 2245 (1966).
(4) J. W. Ledbetter, *J. Phys. Chem.*, **71**, 2351 (1967).
(5) J. W. Ledbetter, *J. Phys. Chem.*, **72**, 4111 (1968).
(6) D. E. Metzler, *Adv. Enzymol.*, **50**, 1 (1979).
(7) D. Heinert and A. E. Martell, *J. Am. Chem. Soc.*, **84**, 3257 (1962).
(8) D. Heinert and A. E. Martell, *J. Am. Chem. Soc.*, **85**, 183 (1963).
(9) D. Heinert and A. E. Martell, *J. Am. Chem. Soc.*, **85**, 188 (1963).
(10) J. W. Ledbetter, *J. Phys. Chem.*, **81**, 54 (1977).

0022-3654/82/2086-2449$01.25/0